THE ASTROPHYSICAL JOURNAL, 256:189–205, 1982 May 1

LITHIUM IN LATE-TYPE GIANTS. II. 31 M GIANTS AND SUPERGIANTS

R. EARLE LUCK
Department of Physics and Astronomy, Louisiana State University
AND
DAVID L. LAMBERT[1]
McDonald Observatory and Department of Astronomy, University of Texas at Austin
Received 1981 August 27; accepted 1981 November 9

ABSTRACT

High resolution, high signal-to-noise spectra have provided Li abundances for 31 M giants and supergiants. The spectrum around the Li I 6707 Å doublet is depressed by unresolved TiO lines. A spectrum synthesis technique was developed to account for the TiO line blanketing and to extract the Li abundance.

The Li abundances in the sample of 25 giants show a large scatter about a mean $\log \epsilon(\mathrm{Li}) \sim -0.2$ with several stars showing no detectable Li or $\log \epsilon(\mathrm{Li}) \lesssim -1.0$. A parallel analysis of the Al I 6696 and 6698 Å lines gives a mean abundance [Al/H] = −0.3 consistent with the idea that the M giants are somewhat older than the Sun. Rediscussion of the Li abundances for G and K giants provides new evidence that the Li abundance in these red giants is primarily controlled by the stellar mass. The M giants generally support this conclusion.

Four of the six M supergiants have the Li/Al ratio expected for rather massive evolved stars. Two (α Ori and 119 Tau) stars show no detectable Li line. The Li deficiency may result from mass loss at the main-sequence phase or internal mixing and nuclear processing leading to Li destruction.

Subject headings: stars: abundances — stars: late-type — stars: supergiants

I. INTRODUCTION

Our understanding of the life cycle of stars and the nuclear reactions which take place within a stellar interior is tested by determining the abundances of those elements which are synthesized or destroyed in the interior and transported to the surface. The elements which are most affected by nuclear reactions and mixing within the star are the light elements. Among these elements, lithium is the species most affected as is made abundantly clear by noting that the observed lithium content of stars spans six orders of magnitude.

The mechanisms which control the lithium abundance have been extensively discussed (see Boesgaard 1976; Luck 1977; Lambert, Dominy, and Sivertsen 1980). The basic idea is that at temperatures of about two million degrees Kelvin the reaction $^7\mathrm{Li}(p,\alpha)^4\mathrm{He}$ destroys lithium. This means that lithium will be destroyed during the main-sequence lifetime throughout the star except in a thin outer shell containing just a few percent of the stellar mass. In addition, if mass loss or semiconvection is active during the main-sequence lifetime, the abundance will be lowered even further, either by removing the lithium from the star or by exposing the lithium to hot protons. When the star ascends the giant branch, convective mixing dilutes the surviving lithium with lithium-free material from the interior. The expected surface abundance of lithium after these processes is at most about 1/30 of the initial abundance with the expected final abundance decreasing with decreasing stellar mass.

Observations of lithium in main-sequence and giant stars, in general, bear out the predicted behavior. Observations of main-sequence stars show that lithium abundances are essentially cosmic in F-type dwarfs (equal to $\log \epsilon(\mathrm{Li}) = 3.0$ on a scale where $\log \mathrm{H} = 12$ [Boesgaard 1976]) decreasing to factor of 0.01 of the cosmic abundance in G- to K-type dwarfs (Herbig 1965; Zappala 1972). Li depletions in dwarfs are more severe than currently predicted by standard models. Semiconvection (Straus, Blake, and Schramm 1976; Schatzman 1977) and turbulent diffusion have been identified as possible agents for enhancing Li destruction. Analyses of G and K giants (Lambert, Dominy, and Sivertsen 1980, hereafter Paper I) show depletions that agree with the standard theory provided that the $^{12}\mathrm{C}/^{13}\mathrm{C}$ ratio of the star in question is normal (say greater than 20), but significantly lower lithium abundances are found if the $^{12}\mathrm{C}/^{13}\mathrm{C}$ ratio is less than 20. A similar result for G and K supergiants was found by Luck (1977).

Lithium abundances in M giants have been determined previously by Merchant (1967) and Boesgaard (1970) from photographic spectra. We undertook a new study of the M giants and supergiants for three reasons. First, Paper I showed that high resolution and signal-to-noise are essential because the Li I 6707 Å doublet is often weak

[1] John Simon Guggenheim Memorial Fellow.

and blended. The advent of new detectors makes it feasible to obtain such data for a large number of M giants. Twenty-five bright M giants and six supergiants were selected and their basic parameters are given in Table 1. Second, the TiO molecule provides a rich curtain of blending lines whose presence should be recognized in the Li abundance determination. In the earlier work, the TiO and other blending lines were ignored. Third, accurate Li abundances with our concurrent analyses of CNO will provide useful constraints of nucleosynthesis and mixing in these stars.

II. OBSERVATIONS

High resolution spectra of the M giants and supergiants were obtained with the McDonald Observatory's 2.7 m telescope, coudé spectrograph, and a Reticon array (Vogt, Tull, and Kelton 1978). A single exposure covered about 25 Å at a resolution of approximately 0.1 Å. The exposure was centered at 6700 Å in order to obtain the Al I doublet at 6696 and 6698 Å as well as the Li I doublet (6707 Å). Typical signal-to-noise ratios were in excess of 100.

In order to obtain a better grasp of the continuum level, moderate resolution spectra (0.2 Å) were acquired for three representative giants and three supergiants. The giants (ν Vir, δ Vir, and HR 5299) were selected to span the temperature range of the program stars. The supergiants 119 Tau, α Ori, and σ CMa were also observed. A single integration of 90 Å length was first acquired for each star. When this proved to be insufficient for accurate continuum placement, additional spectra covering the range 6000 through 7100 Å were acquired and combined. A hot star was also observed at a similar air mass. Division of the spectrum of the M star by that of the hot star removes both the instrumental response and the telluric lines to provide a spectrum of spectrophotometric quality on which the continuum can be reliably interpolated using "windows" spaced far apart.

TABLE 1

BASIC DATA FOR THE PROGRAM STARS

HR	NAME	SPECTRAL TYPE		V	JOHNSON V-K	V-K	Teff	Mv(K)	LOG G	Vm	TIO DEPTH
					GIANTS						
48	7 CET	M0/M3	III	4.46		4.28	3750	-0.9	1.30	3	0.210
337	BETA AND	M0	III	2.05	3.88	3.98	3850	-0.8	1.40	3	0.098
1231	GAMMA ERI	M0.5	III	2.94	3.87	3.90	3875	-0.6	1.55	3	0.069
2275		M1	III	4.89A		4.04	3800	-1.0	1.30	3	0.154
2286	MU GEM	M3	III	2.87	4.76	4.76	3625	-0.7	1.30	3	0.351
2905	UPSILON GEM	M0	III	4.06	3.76	3.79	3900	-0.5	1.60	3	0.041
3288		M1	III	5.95A		4.65	3700	(-0.5)	1.40	3	0.266
3319	27 CNC	M3+	III	5.50	4.96	4.84	3600	(-0.5)	1.30	3	0.379
3705	ALPHA LYN	K7	III	3.13	3.74	3.81	3900	-0.7	1.50	3	0.041
3820		G M1		5.56R		4.06	3800	(-0.5)	1.50	3	0.154
3876		M1.5	III	5.80A		4.15	3775	(-0.5)	1.50	3	0.182
4069	MU UMA	M0	III	3.05	3.93	3.87	3850	-1.0	1.35	3	0.098
4092		M0.5	III	5.56	3.79	3.78	3900	-0.3	1.70	3	0.041
4104	ALPHA ANT	K4.5	III	4.25	3.41	3.34	4000	-0.3	1.60	6	0.000
4434	LAMBDA DRA	M0+	III	3.85	3.99	4.05	3850	-0.1	1.70	3	0.098
4517	NU VIR	M1	III	4.04	3.96	4.04	3825	-0.2	1.65	3	0.124
4910	DELTA VIR	M3	III	3.38	4.63	4.60	3640	-0.4	1.40	3	0.338
5226	10 DRA	M3	III	4.66	4.75	4.84	3625	-0.5	1.35	4	0.351
5299		M4.5	III	5.28	5.65	5.63	3475	-0.4	1.20	6	0.518
5603	SIGMA LIB	M3.5	III	3.27	4.67	4.71	3625	-0.2	1.50	4	0.351
6056	DELTA OPH	M0.5	III	2.75	3.97	4.01	3850	-0.4	1.60	3	0.098
7405	ALPHA VUL	M1	III	4.45	3.90	3.88	3825	-0.5	1.50	3	0.126
7536	DELTA SGE	M2	II	3.83	4.62	4.74	3650	-0.2	1.50	4	0.323
8057		M1	III	6.21R		4.11	3800	(-0.5)	1.50	3	0.154
8080	24 CAP	M1	III	4.49		3.92	3825	+0.3	1.85	3	0.126
					SUPERGIANTS						
1845	119 TAU	M2.1	IAB	4.35	5.24	5.38	3750	-4.8	0.7	8	0.175
2061	ALPHA ORI	M2.2	IAB-	0.42	4.42	----	3900	-5.4	0.0	8	0.145
2197	BU GEM	M1.0	IA	6.11R		5.14	3800		0.0	8	0.240
2646	SIGMA CMA	K5.9	IB	3.43	3.92	3.93	4000	-4.2	1.0	6	0.080
2902	KQ PUP	M2.0	IB	4.98		4.96	3800		0.8	8	0.100
8164A		M1.1	IB	5.68B		4.95	3800		0.8	5	0.190

NOTES.—V magnitudes: No code, Johnson *et al.* 1966; A, Blanco *et al.* 1970; B or R, Hoffleit 1964. Johnson $V-K$, Johnson *et al.* 1966; $V-K$, K magnitude from Neugebauer and Leighton 1969 and V magnitude from fourth column. Effective temperature: Ridgway *et al.* 1980: spectral type-color-temperature calibration. Absolute V magnitude: Wilson 1976 (values in parentheses are assumed values). Gravity: Masses obtained by using luminosity and temperature with evolutionary tracks from Paczyński 1970.

III. THE DETERMINATION OF LITHIUM ABUNDANCES IN M STARS

The stellar parameters of the stars to be analyzed are given in Table 1. Effective temperatures for the giants were obtained by combining the $V-K$ color with the color-temperature relation of Ridgway *et al.* (1980). Tsuji's (1981) application of the infrared flux method gives a similar temperature calibration. The gravities were obtained by placing the stars on evolutionary tracks (Paczyński 1970) using the effective temperatures and absolute magnitudes. The absolute magnitudes were determined from the K line magnitudes of Wilson (1976) with the bolometric corrections of Johnson (1966). The microturbulent velocity was set at 2.5 km s^{-1} for all giants; the exact value is not critical as the Li I feature is never strongly saturated, thanks to the doublet splitting and high thermal velocity.

Parameters for the supergiants (Table 1) were determined by combining results of recent analyses (Luck and Bond 1980; Lambert *et al.* 1981; White 1980) to obtain effective temperatures for 119 Tau, BU Gem, and α Ori. These temperatures were used with the $V-K$ colors to form a temperature-color relation. All stars were taken to be unreddened. Gravities were taken from the above-mentioned references or derived in a manner analogous to that used for the giants. A microturbulence of 4.0 km s^{-1} was used for all supergiants.

Model atmospheres were taken from the grid by Johnson, Bernat, and Krupp (1980). These models are line-blanketed and include TiO. They represent the state-of-the-art in model building for M stars. (Note the model atmosphere grid provided by Gustafsson *et al.* 1975 is not appropriate because the TiO line blanketing is not included.) The Li abundance is fairly sensitive to temperature, and the temperature structure could be adversely affected by failure of core assumptions such as LTE and plane-parallel geometry in the models. We shall return at a later point to these concerns.

Oscillator strengths for the Al I 6696 and 6698 Å doublet were derived using an inverted solar analysis. The equivalent widths were measured from the *Liège Atlas* (Delbouille, Nevin, and Roland 1973). The inversion was performed using the Holweger solar model (Holweger 1967; Holweger and Müller 1974) with a depth independent microturbulent velocity of 1.0 km s^{-1}. The Al abundance was taken to be that recommended by Lambert and Luck (1978). Atomic lines of other species were handled in the same manner except that their equivalent widths were from Moore, Minnaert, and Houtgast (1966). For lines not present in the solar spectrum but, in all probability, observable in an M giant, line parameters were taken from Kurucz and Peytremann (1978). Absolute oscillator strengths for Li I were taken from Wiese, Smith, and Glennon (1966).

Two molecules–TiO and CN–contribute lines. The CN red system lines near 6700 Å are very weak in M giants. We have included in the syntheses all CN lines given by Davis and Phillips (1963) using a band oscillator strength $f(0, 0) \equiv 1.1\ (10^{-3})$ and the relative oscillator strengths of Arnold and Nicholls (1972). The adopted CNO abundances were 8.4, 8.4, and 8.9, which are typical of processed giants. The spectrum is dominated by TiO. Relative line strengths (Hönl-London factors) were computed using the code of Whiting (1972). We adopted $f(0, 0) = 4\ (10^{-3})$ for the γ system and calculated $f_{v'v''}$ for other bands from Franck-Condon factors (Collins and Faÿ 1974) and an assumption that the electronic transition moment is constant. This procedure yielded Ti abundances near solar when TiO features were synthesized with our initial choice of continuum. The primary TiO contribution in the 6700 Å region comes from the (1, 0) band of the γ system with minor contributions from other bands of the $\Delta v = +1$ and $+2$ sequences. Isotopic lines of ^{46}TiO, ^{47}TiO, ^{49}TiO, and ^{50}TiO were also included in the synthesis for lines of the (1, 0) band in addition to the main isotope ^{48}TiO. The isotopic abundance ratios were assumed to be terrestrial (see Clegg, Lambert, and Bell 1979). The wavelengths of the main isotope lines were from Phillips (1973) (as taken from a tape kindly supplied by Professor Phillips), and the isotope shifts were computed from the molecular constants (Phillips 1973).

The Li abundance was extracted by spectrum synthesis. This technique has been previously exploited (Luck 1977; Paper I) for the determination of lithium abundances. Both studies synthesized only a limited region about the lithium doublet (typically 1.5 Å to either side). As the M stars are more heavily blended than the G or K stars previously studied, we decided to synthesize an expanded region about the lithium feature in order to check continuum placement and overall quality of the synthetic spectrum. We synthesized the 17 Å region 6694 through 6711 Å. This region not only includes the lithium doublet but also a pair of Al I lines which serve as a control because the Al abundance is not expected to change during the evolution from main sequence to red giant.

The TiO molecule contributes by far the larger portion of absorption in the observed spectral region. We first matched this absorption using the Ti abundance as the free parameter changing the abundance until the depth of unblended (that is, unblended with atomic features) TiO features were matched. Then, the atomic lines were added and matched to the observed spectrum using the oscillator strength as the free parameter; for Al and Li we adjusted the abundance. The macroturbulence was found by trial and error fitting of relatively unblended lines. We assumed a Gaussian distribution of macroturbulent velocity. The final result is a best-fitting spectrum which has most features matched (minor mismatches are inevitable) from which the unblended strengths of Li and Al can be extracted. The use of *gf* values allows several lines of the same species to be varied independently to obtain a best match. If, at the end, an abundance is desired from a *gf*-matched feature, it is easily obtained by comparing the "matching" *gf* value to the absolute *gf* value.

Continuum placement was initially determined by inspection of a 0.2 Å resolution spectrum spanning 90 Å

around the Li I doublet. The highest points of the echelle spectra were also among the highest points of the moderate resolution spectra suggesting that these points may approach the "true continuum." Therefore, the continuum was given a constant value over the entire 17 Å region to be synthesized at the level of the highest point (the flux difference expected from a 3800 K, log g model over the 17 Å is less than 1%). This point was the same in all spectra and is at a wavelength of 6710.7 Å. The region was then synthesized in all giants and plausible fits were achieved. However, the derived aluminum abundances decrease sharply with decreasing temperature (Fig. 1). The order of magnitude change in abundance corresponds to a 400 K change in effective temperature. This unexpected result suggested that the initial analysis was in error. Several possible ideas were considered. The effect is unlikely to be real because the space motions of the sample are not representative of metal-poor disk stars. As noted above, the Al abundance is not expected to be changed by nuclear processing and mixing.

The temperature scale is a possible source of error. However, a gross error (400 K) is needed to remove the abundance trend with temperature. If this correction were applied, the M3 and M4 III giants would have similar temperatures to the early M stars, but the color indices clearly require a significant temperature span from M0 to M4 and beyond. Further, a change in scale leading to an approximately constant temperature change for all M giants would primarily shift all abundances upward and downward and roughly preserve the temperature dependence. Therefore, the adopted temperature scale is unlikely to cause the observed abundance trend.

The placement of the continuum in a M giant is a difficult task. The primary problem is the general overlying haze arising from myriad TiO lines. As the temperature decreases the absorption increases greatly in strength, and the continuum placement becomes increasingly difficult. If the local high points are depressed by the TiO haze, the equivalent widths will be underestimated in the coolest stars, and hence, the abundances are underestimated. This is precisely the observed trend in the Al abundances.

As a check upon the continuum placement, we obtained moderate resolution spectra covering 6000–7100 Å for three giants. These spectra provide relative fluxes over the entire interval. By inspection, it is immediately obvious that the entire region covered by our original 90 Å wide spectra is depressed and that the adopted continuum point is depressed in the coolest stars by amounts exceeding 20% from the interpolated continuum (Fig. 2). The latter was arrived at by considering the highest intensity points outside the strongest TiO bandheads. Of course, even these points may be depressed by a weak haze of lines. After obtaining the depth of a specified point (6710.7 Å) in each of the three giants, we found that the depth-effective temperature relation was linear. We used this linear relation to assign the continuum to all other stars. The last column in Table 1, headed "TIO DEPTH," is the amount by which the highest point in the echelle spectra (6710.7 Å) is depressed relative to the continuum.

With the new continuum placement, syntheses were performed for several stars. It was immediately determined that in no case could an adequate fit be found. If the line depths were matched, the regions of "local continuum" such as 6710.7 Å were not depressed;

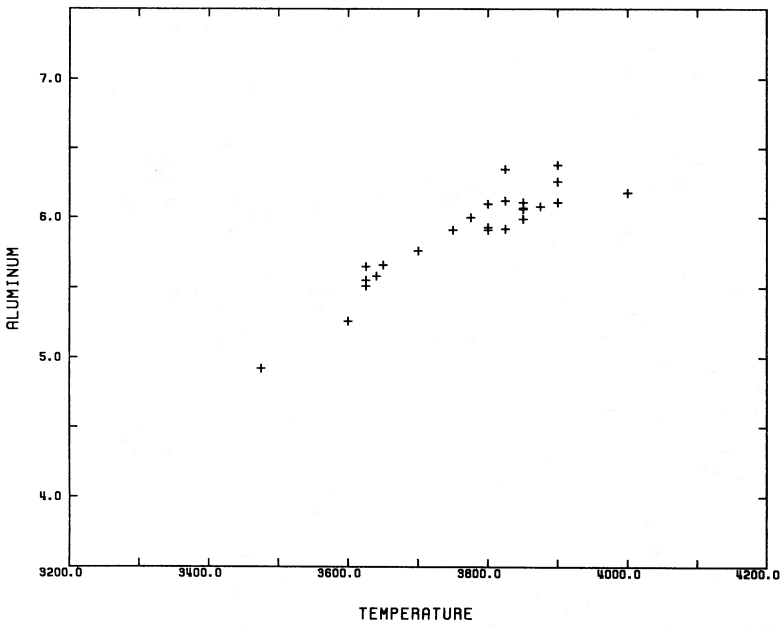

FIG. 1.—The abundance of aluminum in M giants vs. effective temperature. The aluminum abundances were determined relative to a continuum placement obtained based on inspection of the local 90 Å region about 6700 Å.

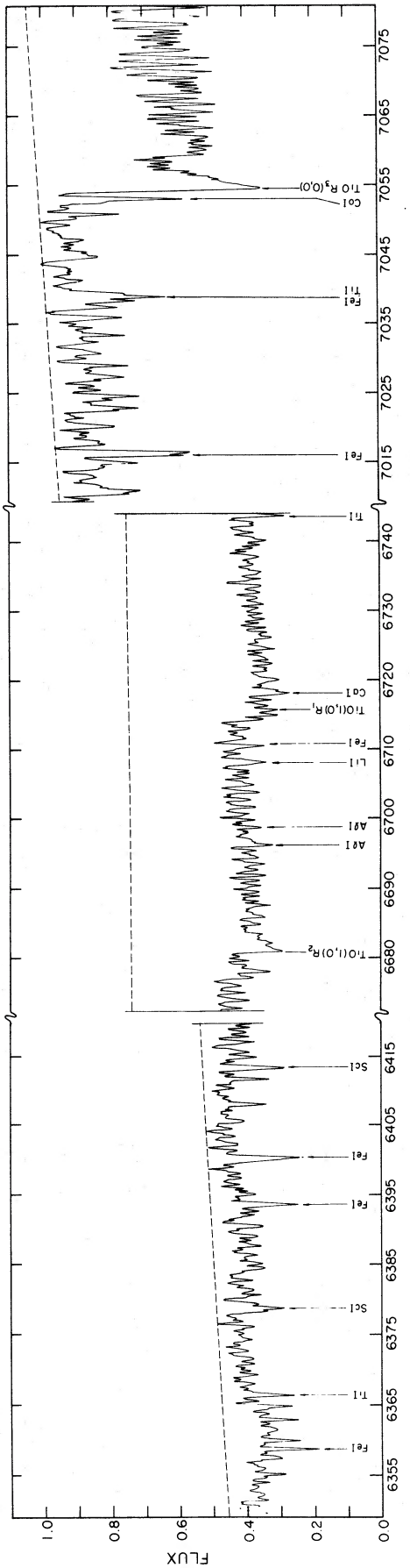

FIG. 2.—A relative flux spectrum of δ Vir showing two regions bracketing the region 6700 Å which approach continuum. The solid line indicated shows the continuum level used in the analysis.

the synthetic spectra attained nearly the level of the true continuum. This mismatch is attributable to an inadequate TiO line list. For example, the γ'-system crosses this region, but such lines have not been analyzed and included in the available line lists. Even if we could include all lines of these other systems in the synthesis, an already unwieldy problem would be made impossible.[2] The solution settled upon was to treat the missing lines as a single giant TiO line which is frequency independent and whose depth is specified in the calculation. The assumed lower potential for the line is 1.0 eV. Since the previous calculations with the proper continuum showed that the synthetic spectra without the giant line rise to intensity level about 1.0 at 6710.7 Å (where "TIO DEPTH" is specified) we assume that the giant TiO line supplies the entire depression. To maintain the strength of the giant line feature at a constant value, we modify its "*gf*" value each iteration (if necessary) until the proper depth is achieved. The synthesis is then performed adding the giant TiO line to each wavelength point by treating it as another line whose strength is fixed.

With this procedure the syntheses were repeated and satisfactory agreement was obtained between the synthetic and observed spectra. In Figure 3, we show a series of synthetic and observed spectra for a range of effective temperatures and lithium strengths. The actual temperature range of the stars is quite small (most stars have temperatures within 200 degrees of 3800 K), but the TiO depression dependence upon temperature is quite steep. The best syntheses are those at temperatures in excess of 3800 K where the depression is 15% or less. As the temperature decreases, there are increasing mismatches in the spectra as the continuum placement becomes more uncertain. Given the complexity of the situation, we feel that it is very pleasing that fits as good as these can be obtained.

Inspection of Figure 3 also shows that lithium exhibits a wide range of strengths in these stars. In stars with weak lithium (Fig. 3*a*) it is obvious that high resolution and signal-to-noise are essential as the blending lines (both atomic and molecular) in many cases are stronger than the lithium component.

No matter how aesthetically pleasing our syntheses may be, the key question is: What are the aluminum abundances? They are shown in Figure 4. Aluminum is now constant with respect to temperature and shows a mean [Al/H] ratio of -0.3 dex. The lack of temperature dependence is precisely the desired result. Furthermore, the mean [Al/H] ratio agrees well with that expected from extrapolation of metallicities in G and K giants. Therefore, we must conclude that our placement of the continuum and the treatment of the giant TiO line is basically correct and that the analysis of the M giants is now internally consistent. From the syntheses we have extracted equivalent widths and abundances for Li and Al. Data on these species can be found in Tables 2 and 3.

A similar analysis was performed for the M supergiants. We obtained spectra covering the region 6000–7100 Å in three supergiants and find that the region around 6700 Å is depressed much as it is in the giants. We set the continuum using the same criteria as used for the giants. The strength of the depression at 6710.7 Å is given in Table 1. Performing the syntheses using the giant TiO line to account for the entire depression left the overall spectrum mismatched due to inadequate strength in the resolved TiO γ (1, 0) lines. The problem is that the large macroturbulent velocity found in the supergiants smears the spectrum to such a degree that the high intensity points are lowered not merely by the background haze, but, also, by the macroturbulence itself. Thus, the unblended weak TiO features [such as $R_2(58)$ 6707.130] are essentially unresolved. If these lines are used to derive the TiO strength, the stronger Q-branch lines are too weak. The presence of the giant TiO line effectively forms a local continuum with respect to which the remaining lines can be measured. Thus, we can ask what must the depth of the giant line be to give consistent depths between the Q- and R-branch lines of γ (1, 0) TiO. In the giants this depth is just the measured depression,

TABLE 2

EQUIVALENT WIDTHS

HR	Star	Lithium Doublet (1)	Lithium Doublet (2)	Al I λ6698
48	7 Cet	92	173	71
337	β And	28	58	90
1231	γ Eri	195	315	87
2275		84	123	82
2286	μ Gem	42	...	46
2905	υ Gem	29	...	106
3288		49	119	58
3319	27 Cnc	14	...	28
3705	α Lyn	46	70	91
3820		4	39	74
3876		79	147	79
4069	μ UMa	84	97	84
4092		9	23	107
4104	α Ant	34	...	95
4434	λ Dra	11	...	76
4517	ν Vir	5	46	67
4910	δ Vir	72	197	43
5226	10 Dra	3	...	47
5299		11	...	28
5603	σ Lib	25	109	48
6056	δ Oph	8	75	89
7405	α Vul	8	71	88
7536	δ Sge	152	350	47
8057		80	111	68
8080	24 Cap	12	38	97

NOTE.—All equivalent widths less than 10 mÅ should be considered as upper limits.

REFERENCES.—(1) This study. (2) Merchant 1967.

[2] The line list in its current form has some 600 lines in the 17 Å. The wavelength step used is 0.01 Å. A single iteration toward the desired spectrum takes 5 CPU minutes on an IBM 3033 computer, and typically six iterations are needed to match most of the more than 25 separate features in the spectrum.

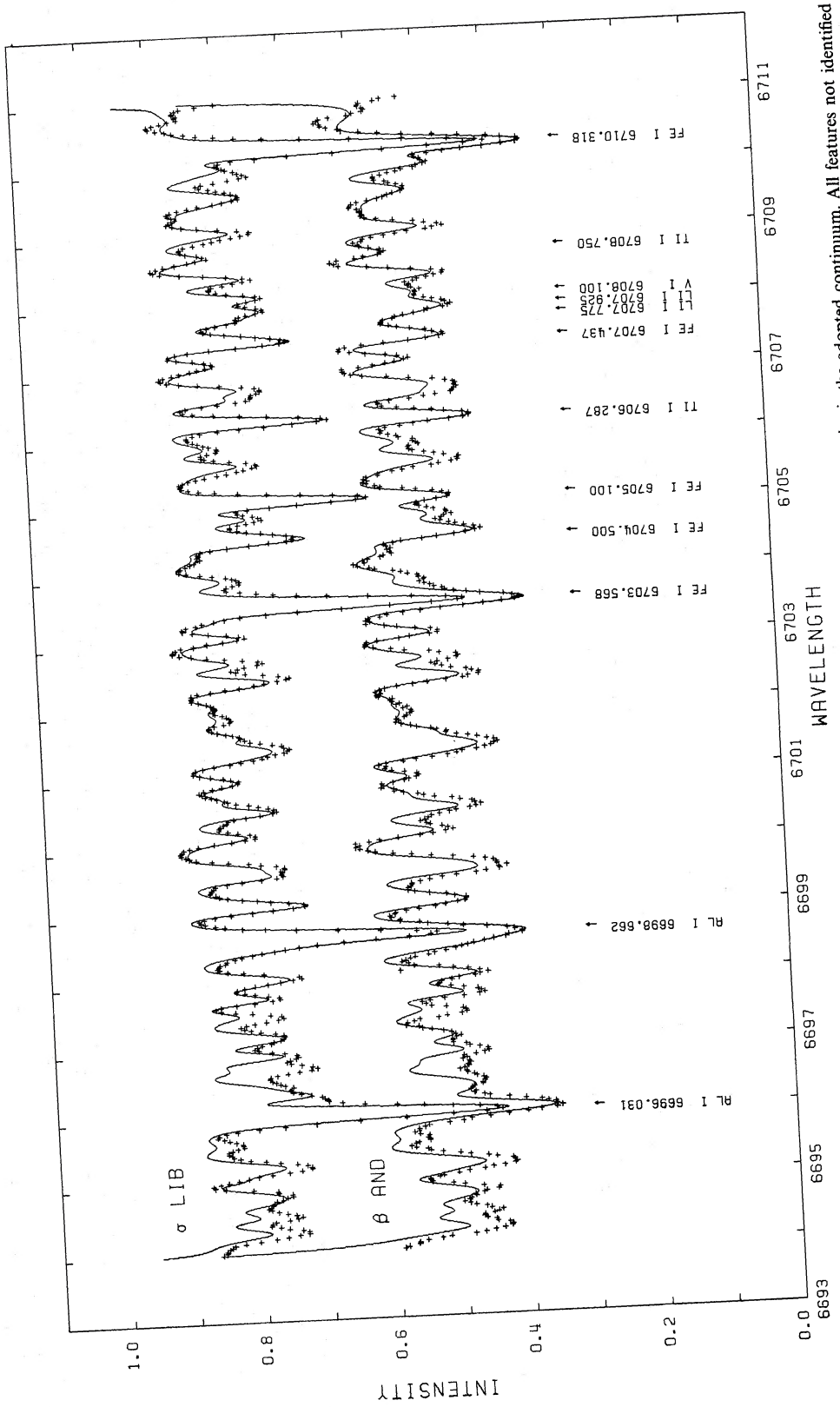

FIG. 3.—Syntheses of 6694–6711 Å in giants of various temperature and lithium strength. In all cases the 1.0 intensity is the adopted continuum. All features not identified have as their principal component TiO.

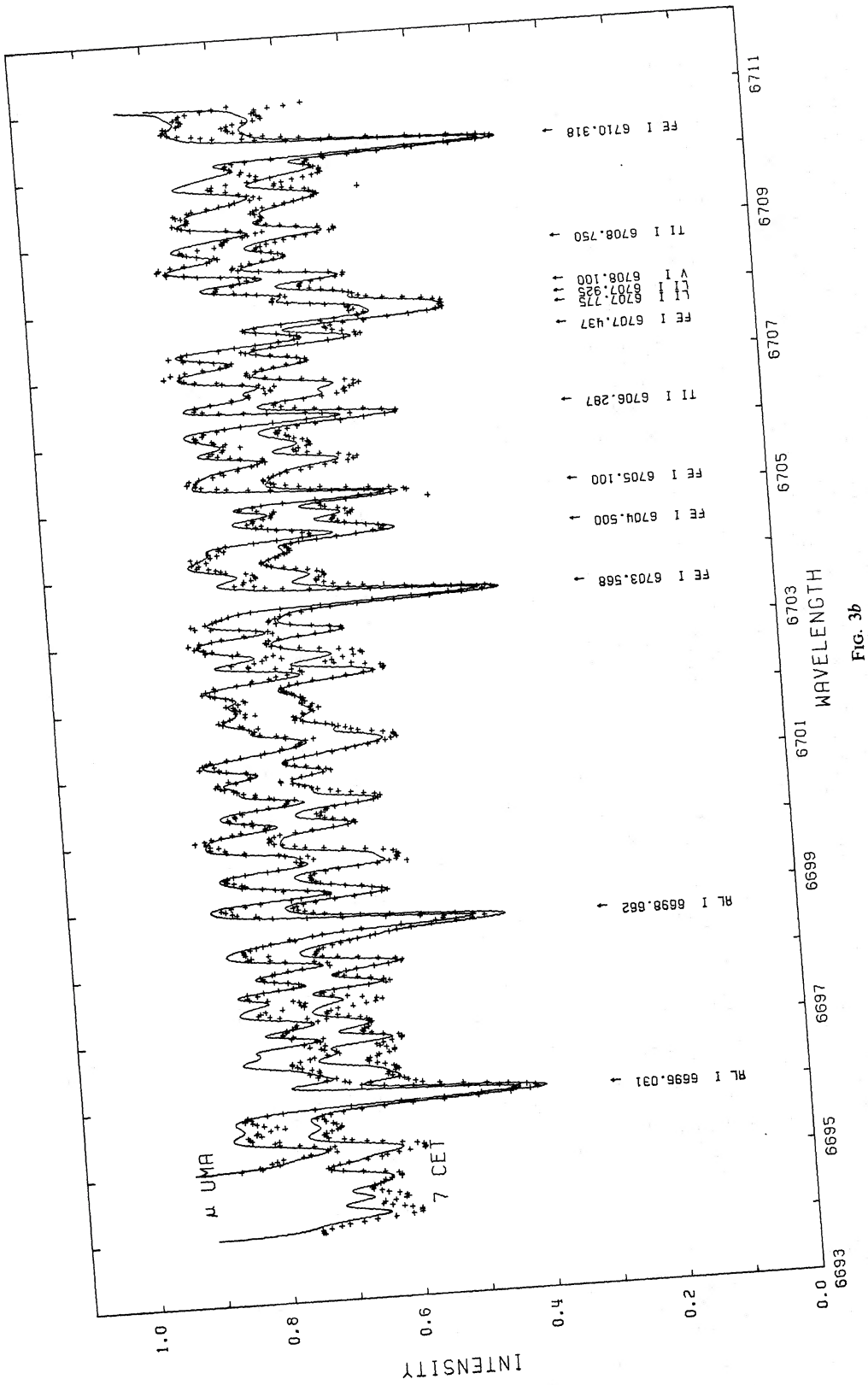

FIG. 3b

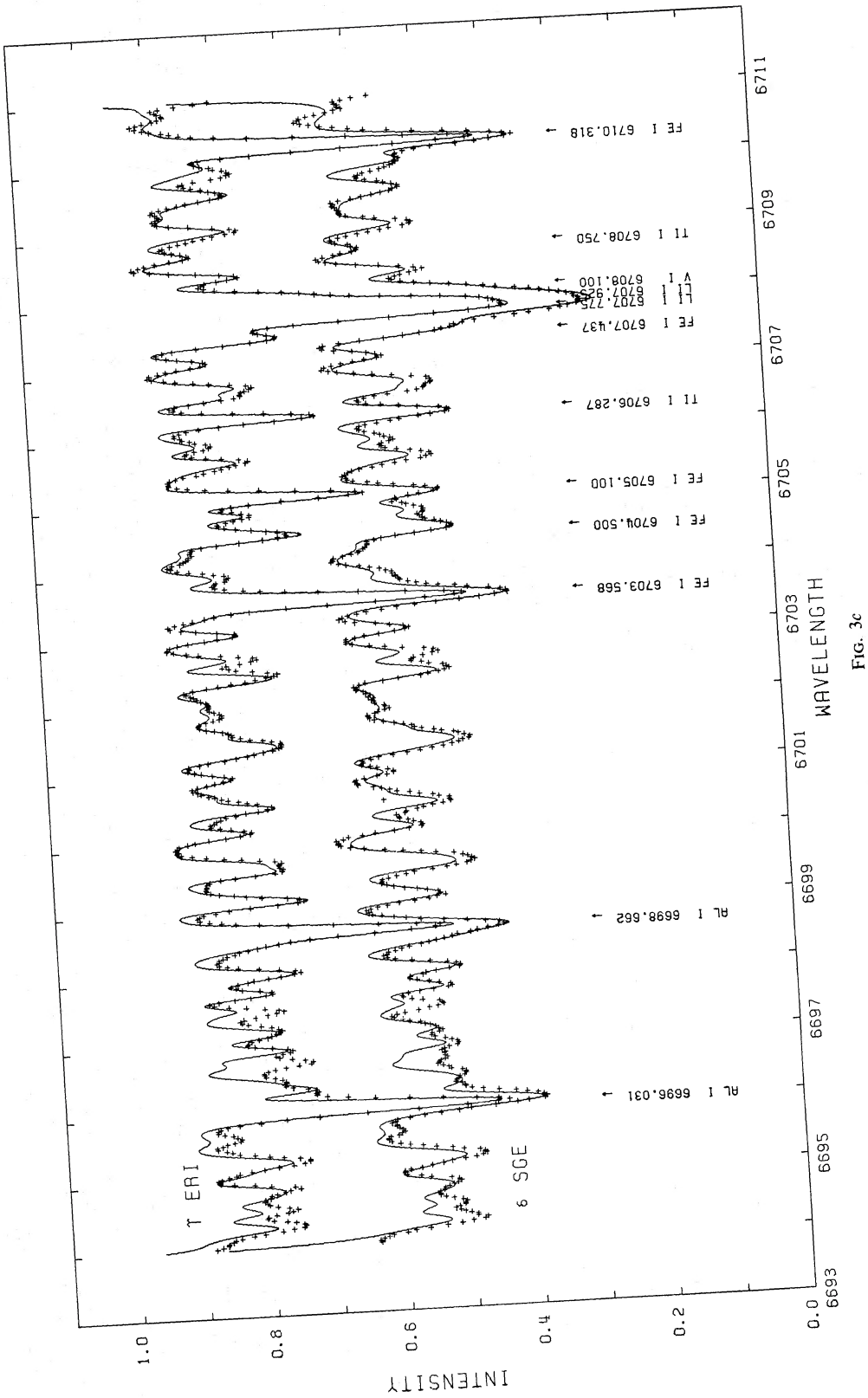

FIG. 3c

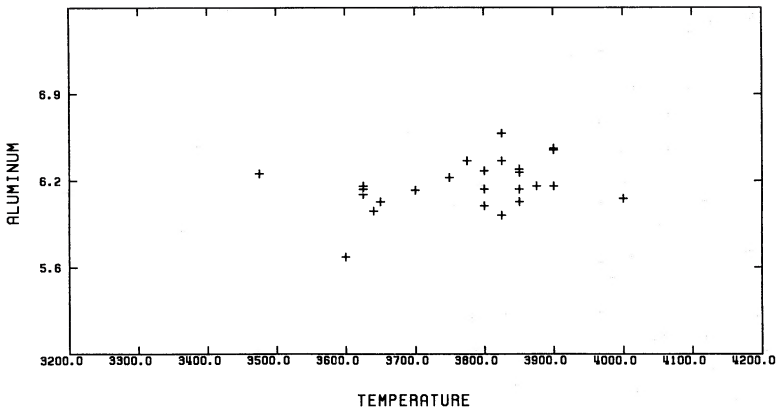

FIG. 4.—The abundance in M giants vs. effective temperature. The aluminum abundances were determined relative to a continuum placement based on inspection of a baseline extending from 6000–7100 Å.

but in the supergiants the depth is somewhat less than the total depression.

The supergiant syntheses shown in Figure 5 have been performed using the total continuum depressions given in Table 1 and the giant line depths given in Table 4. As can be seen, the fits are adequate. Table 4 gives the computed equivalent widths and abundances for lithium and aluminum in the six supergiants. Note that a lower resolution spectrum (0.2 Å) was used for BU Gem.

TABLE 3

LOGARITHMIC ABUNDANCES FOR M GIANTS

HR	Name	Li	Al
48	7 Cet	+0.18	6.27
337	β And	−0.48	6.33
1231	γ Eri	+0.80	6.21
2275		+0.11	6.32
2286	μ Gem	−0.26	6.15
2905	υ Gem	−0.45	6.47
3288		−0.20	6.18
3319	27 Cnc	−0.82	5.70
3705	α Lyn	−0.21	6.21
3820		≤ -1.22	6.19
3876		+0.08	6.39
4069	μ UMa	+0.13	6.19
4092		≤ -1.02	6.48
4104	α Ant	−0.24	6.12
4434	λ Dra	−0.89	6.10
4517	ν Vir	≤ -1.28	6.00
4910	δ Vir	+0.09	6.03
5226	10 Dra	≤ -1.50	6.19
5299		≤ -0.87	6.30
5603	σ Lib	−0.55	6.21
6056	δ Oph	≤ -1.19	6.31
7405	α Vul	≤ -1.08	6.39
7536	δ Sge	+0.84	6.10
8057		+0.15	6.07
8080	24 Cap	−0.87	6.59
MEAN		...	6.22
σ		...	0.18
[M/H]		...	−0.27

NOTE.—All abundances are logarithmic with respect to log ϵ(H) = 12.

IV. RESULTS

Our study demonstrates that syntheses of M giants can be performed and that, with adequate care, an abundance analysis is possible. Obviously, the uncertainty in the analysis is probably dominated by the placement of the continuum. Here, we shall first discuss the abundance results and, then, the uncertainties associated with them.

Lithium abundances for the giants are given in Table 3 and are plotted against effective temperature in Figure 6. As can be seen, the derived abundances (and limits) scatter widely; the actual range is from +0.84 dex to −0.89 dex. The measurements (upper limits excluded) have a mean value −0.2 dex (relative to H = 12). This mean is a factor of 1600 below the accepted cosmic abundance. Clearly, all of the stars have suffered severe lithium depletions during their lifetimes.

The abundance limits shown in Figure 6 are derived from the equivalent widths given in Table 2. We consider any equivalent width less than 10 mÅ to be a limit on the equivalent width. For the supergiants we consider 25 mÅ

TABLE 4

EQUIVALENT WIDTH AND ABUNDANCE DATA FOR M SUPERGIANTS

		LITHIUM		ALUMINUM	
STAR	TiO[a]	W_λ[b]	log ϵ	W_λ	log ϵ
119 Tau	0.130	22	≤ -0.66	110	6.10
α Ori	0.145	11	≤ -0.88	64	5.65
BU Gem	0.240	92	+0.15	60	5.66
σ CMa	0.080	98	+0.30	123	6.19
KQ Pup	0.100	135	+0.29	104	5.98
HR 8164A	0.190	123	+0.35	85	5.96

NOTE.—These equivalent widths and abundances have been computed using a significant TiO background opacity. All abundances are logarithmic with respect to log ϵ(H) = 12.

[a] The depth of the "giant line" (see text) used to compute the abundances. The overall continuum height is that given in the last column of Table 1.

[b] The W_λ given for Li refers to the entire doublet.

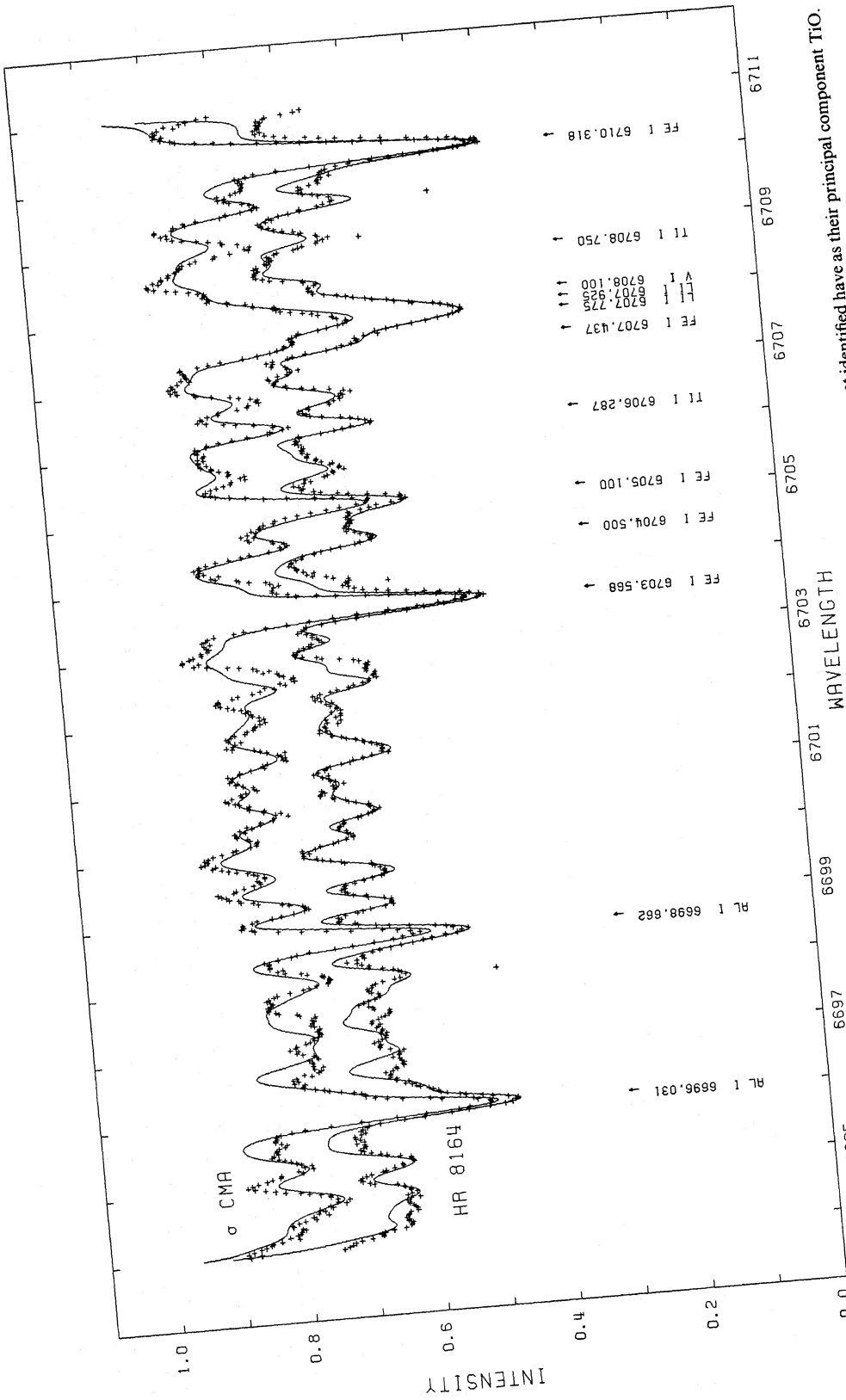

FIG. 5.—Syntheses of 6694–6711 Å in two supergiants. In both cases the 1.0 intensity is the adopted continuum. All features not identified have as their principal component TiO.

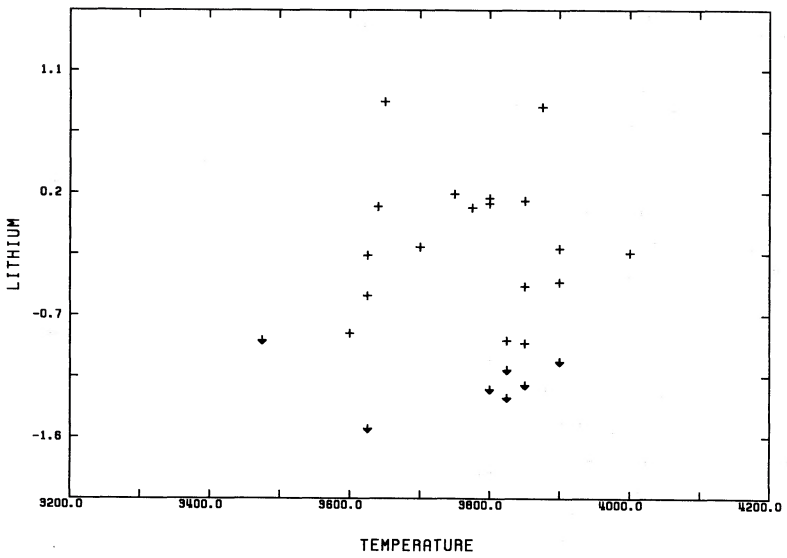

FIG. 6.—Lithium abundances in the M giants vs. effective temperature. Upper limits are denoted by the inverted arrow.

to be the smallest detectable equivalent width. Also, our calculations refer only to ^{7}Li. In no case was there any evidence of the presence of ^{6}Li. However, the search for ^{6}Li is hampered by the coincidence of both lines of the doublet with intervening lines. The stronger ^{6}Li line is coincident with the weaker line of the ^{7}Li doublet as well as a Q-branch line of ^{48}TiO γ (1, 0). The weaker ^{6}Li line is blended with a low potential V I line. As discussed by Luck (1977) and in Paper I, the presence of these interfering lines confuses the determination of lithium isotope ratios.

Our analysis of the supergiants appears to be afflicted by a systematic error because the Al abundances are significantly below the solar value, $\log \epsilon(\mathrm{Al}) = 6.49$ according to Lambert and Luck (1978). For example, α Ori has $[\mathrm{Al/H}] = -0.84$, but analysis of metal lines in the near-infrared show that the metal abundance is, as expected, solar or slightly in excess of solar (Lambert *et al.* 1981). We suspect that the continuum at 6700 Å has been set too low. In our discussion, we shall consider the Li/Al ratio which is less sensitive to a continuum misplacement.

As a check on possible systematic errors in the lithium abundances, it is customary to determine the abundance of another species whose accessible lines show an approximately Li-like sensitivity to the atmospheric structure but whose abundance is immune to the nuclear processing and mixing affecting lithium. For this purpose, we have used the aluminum doublet. Most previous studies have used calcium. In Paper I, we employed the Ca I line at 6798 Å. In M stars, this line is not very suitable because it is redward of all three ^{48}TiO (1, 0) γ system bandheads so that the continuum depression is larger. The close proximity of the Al doublet to the Li feature is an advantage when continuum placement is a major problem. The aluminum abundances of the giants have already been discussed; Figure 4 demonstrates the lack of a temperature abundance correlation. We have also determined iron abundances from three lines of differing lower potential. The abundances predicted by these lines also show no dependence upon effective temperature. We note that the three iron lines yield a mean abundance which is within a factor of 2 of the metallicity implied by the aluminum abundance. The scatter is large (± 0.2 dex) on a line-to-line basis. However, there are large uncertainties with regard to blending and the gf-values which lead to a larger scatter than one might normally expect. The absence of an abundance-temperature trend is pleasing.

Two parameters which have only relatively minor influences on the abundances are gravity and microturbulent velocity. Note that even if the lithium doublet attains an equivalent width of several hundred mÅ that it is not strongly saturated as the doublet splitting and large thermal velocity effectively desaturate the line. The sensitivity of the abundances to these parameters is explicitly set out in Table 5.

The primary uncertainty in these abundances is the placement of the continuum. The effect that this can have

TABLE 5

SENSITIVITY OF ABUNDANCES TO PARAMETERS

Species		ΔT 3800 → 4000	$\Delta \log G$ 1.0 → 1.5	ΔVt 2.5 → 3.5
Li I.....	15 mÅ	+0.29	+0.03	−0.01
	75 mÅ	+0.29	+0.02	−0.03
	150 mÅ	+0.26	+0.03	−0.07
Al I.....	80 mÅ	+0.05	+0.05	−0.18

NOTE.—Quoted equivalent width refers to entire lithium doublet. The fixed parameters for the changes are: ΔT: $\log G = 1.5$ and $Vt = 2.5$ km s^{-1}; $\Delta \log G$: $T_{\mathrm{eff}} = 3800$ K and $Vt = 2.5$ km s^{-1}; and ΔVt: $T_{\mathrm{eff}} = 3800$ K and $\log G = 1.5$.

on the abundances is demonstrated by comparing Figures 1 and 4 where the aluminum abundances determined from two different continuum placements are shown. The absolute placement of continuum remains uncertain. The constancy of the derived abundances of Al and Fe argues that the placement within this group of stars is consistent. If the placement were in error, the most likely sense would be that the placement is too low with the error increasing with decreasing effective temperature. However, a higher placement would cause differential effects within the abundances, i.e., the abundances within the cooler stars would be raised over those of the warmer stars creating a new abundance-temperature correlation. This would be as unpalatable as our initial correlation. Therefore, we feel that the continuum placement is accurate to within a tolerance level of approximately 5%, that is, on the normalized scale shown in Figures 2 and 4, the continuum is between 0.95 and 1.05. This contributes an uncertainty of order ± 0.2 to the Li abundance. The error in the Li/Al abundance ratios is smaller ($\approx \pm 0.1$ dex).

Another check on the assigned continuum is the electronic oscillator strength of TiO γ (0, 0). The final fit Ti abundances are substantially above solar [this is because the continuum was raised but $f(0, 0)$ was left unaltered], so the value of $\gamma f(0, 0)$ is a corresponding factor too low. Setting the titanium abundance to the value implied by [Ti/H] = [Al/H], one can derive the implied "absolute" oscillator strength. The mean value obtained for the 25 giants is 0.053 (error in the mean ± 0.009). The best laboratory data available (Price, Sulzman, and Penner 1974) returns a value 0.31 ± 0.12. Consideration of all sources of information (both laboratory and stellar) lead Bell and Gustafsson (1978) to adopt 0.05 as the best value for $^{48}\mathrm{TiO}(\gamma) f(0, 0)$. We have retrieved precisely this value for these M giants using a "blind" approach. This gives us greater confidence in the assigned continuum and the corresponding TiO strengths implied by that placement.

A potentially serious deficiency of the models is the failure of the core assumption of LTE with respect to the ionization of the elements with a low first ionization potential. These include major contributors to the electron pressure and, of course, Li and Al. Auman and Woodrow (1975) noted that there should be no major corrections to the model atmospheres themselves until the effective temperature falls below 3500 K; the electron donors are almost fully ionized in LTE. However, the abundances computed from neutral species of low first ionization potential may be significantly in error, thanks to overionization. Lithium and aluminum are such elements. Calcium also has a low first ionization potential, and Ramsey (1977, 1981) has presented empirical evidence for significant non-LTE perturbations in Ca I, particularly for effective temperatures less than 4000 K. He uses the line pair Ca I 6572 Å and [Ca II] 7323 Å. Unfortunately, continuum placement in an M giant or supergiant is difficult. This pair both fall in heavily depressed regions, so that the line ratio as used is most probably unreliable. Also note that Ramsey apparently used a local continuum which, as we have shown, is quite inadequate.

Luck (1977) reported statistical equilibrium calculations for Li in G and K supergiants finding departures from LTE at effective temperatures less than 4500 K. However, these effects are controlled by the flux at wavelengths less than 4000 Å. We repeated the calculation using Luck's model atom, the Johnson, Bernat, and Krupp (1980) models, and the Auer, Heasley, and Milkey (1972) non-LTE line transfer code adapted for use in cooler atmospheres and now including an empirical line-blanketing. For computational ease, we used the solar line-blanketing scheme of Mutschlechner and Keller (1972) scaled by a factor (1/30) as appropriate for late-type giants (Johnson *et al.* 1977). We also used other scalings to test the sensitivity of the non-LTE effect to the strength of the line-blanketing. Comparing the non-LTE results with LTE values for fixed line strengths, we find no abundance difference larger than 0.1 dex. The line-blanketing reduces the flux of ionizing photons and maintains the ionization of Li close to the LTE level. We suggest that non-LTE effects are not important in the ionization of lithium (and probably aluminum too) in early M giants and supergiants. This conclusion can be extended to G and K Ib stars; and therefore, the non-LTE results of Luck (1977) should not be used. The LTE values of Luck are accurate to the stated limits and should be used in discussion of lithium abundances.

Many of the giants considered in this study were first analyzed by Merchant (1967). A direct comparison of equivalent widths is given in Table 2. As can be seen, our results are always less than those of Merchant. The Merchant values are directly measured values from 4 to 16 Å mm^{-1} plates using a local continuum and including the contribution from lines blended with the Li I doublet. Our equivalent widths have been determined from spectrum syntheses allowing for blending with TiO, Fe, and V and the TiO quasi-continuous opacity. Figure 2 shows that these blending components are significant. We suggest that our equivalent widths are greatly improved over those of Merchant. The actual derived abundances are not vastly different, however. This is because the Merchant study used much lower temperatures which compensated for her use of larger equivalent widths. Since we have used improved equivalent width and temperature data, our abundances should be more reliable.

In summary, we find lithium abundances in our selection of objects ranging from $+0.84$ to -0.89 dex with a mean abundance of about -0.2 for the M giants. Several stars show no detectable Li with the upper limits on the abundance extending as low as $\log \epsilon(\mathrm{Li}) < -1.5$ (10 Dra). The constancy of the Al and Fe abundances as a function of temperature argues against any significant temperature effects in the data. The abundances of all three elements are predicted to be insensitive to the adopted surface gravity. The primary uncertainty lies in the placement of the continuum and enters at the level of ± 0.2 dex in the abundances. From detailed statistical equilibrium calculations for lithium,

we find no evidence for significant non-LTE effects in the abundances. We estimate the total uncertainty in any individual abundance to be ± 0.3 dex. An abundance ratio such as Li/Al should be somewhat more accurate.

V. DISCUSSION

Our interpretation of the Li abundances is based on the idea that Li is destroyed during the main sequence phase and the surviving Li in the outer envelope is further diluted in red giants by a deep convection zone. A detailed discussion of the predicted Li abundances for red giants was given in Paper I.

a) *The M Supergiants*

The six supergiants are surely rather massive stars. For $\mathcal{M} \geq 3\ \mathcal{M}_\odot$, a Li abundance $\log \epsilon(\mathrm{Li}) \sim 1.2$ is predicted from Iben's (1966) models for main-sequence and red giant stars. If we consider the Li/Al ratio (see § IV) and assume that these stars possess a solar Al abundance, the four supergiants with a detectable Li line (i.e., $W_\lambda \geq 25$ mÅ) provide a mean abundance $\log \epsilon(\mathrm{Li}) = 0.82$. This is a factor of 2 below the prediction. While this difference might just be attributable to the observational uncertainties, the Li deficiency might reflect one or more of the following factors:

1. These very young stars have a small Al overabundance.

2. Mass loss prior to the red giant phase would reduce the Li-containing outer skin and lead to a reduced Li abundance as a convectively mixed red giant. A mass loss rate of $10^{-8}\ \mathcal{M}_\odot\ \mathrm{yr}^{-1}$ would remove $0.2\ \mathcal{M}_\odot$ (or 2%) from a $10\ \mathcal{M}_\odot$ star during its main-sequence lifetime and cut the Li abundance in the red giant by at least a factor of 2. Observed mass loss rates (see the review by Cassinelli 1979) certainly exceed this required rate. Indeed, the puzzle may be to explain why any Li is seen in these supergiants!

3. The interior structure of the real stars may differ from the model structures. For example, rapid rotation may induce a circulation which could destroy more Li in the main sequence phase.

For the two stars, 119 Tau and α Ori, with no detectable Li, the observed abundance limit is about a factor of 20 below the standard predictions. In addition, α Ori shows an excess ^{13}C abundance: $^{12}\mathrm{C}/^{13}\mathrm{C} \approx 7$ is observed (Hinkle, Lambert, and Snell 1976; Bernat *et al.* 1979), but $^{12}\mathrm{C}/^{13}\mathrm{C} \approx 20$ is predicted. (A ^{13}C analysis has not yet been completed for 119 Tau.) Severe mass loss or a mixing process in the interior could remove/destroy Li and reduce the $^{12}\mathrm{C}/^{13}\mathrm{C}$ ratio. A full element and isotopic abundance analysis for the CNO trio might provide a discriminant between these two (and other) possibilities. Our sample of supergiants is too small but inspection of Merchant's (1967) slightly larger sample suggests that Li in these stars may run down from $\log \epsilon(\mathrm{Li}) \approx 1.0$ to $\log \epsilon(\mathrm{Li}) \approx -0.3$ and below. It would be of interest to examine a larger sample (e.g., the h and χ Per cluster supergiants) in order to determine the distribution function for the Li abundance and other indicators of nuclear processing and mixing.

b) *Giants of Spectral Types G, K, and M*

Paper I presented a simple argument predicting that the Li abundance of a red giant should be dependent on the stellar mass provided that the real and model stars are similar. There were two major components to the argument. First, observations of main-sequence stars indicate that their surface abundance decreases with increasing age (Zappala 1972; Duncan 1981). Second, red giant models predict that the dilution of the surface Li is a (weak) function of mass. The Li-mass relation for red giants was not tested extensively in Paper I. Before examining our new results for the M giants, we present a new discussion of the Li abundances from Paper I.

Direct estimates of the stellar mass are available for very few red giants. We obtained relative masses for the G and K giants from their location in the H-R diagram. Effective temperature estimates were taken from Paper I. Bolometric magnitudes were computed from the Ca II K line absolute visual magnitudes (Wilson 1976) and predicted bolometric corrections (Gustafsson and Bell 1979). For a fixed composition, the evolutionary tracks for different masses are almost parallel (see, for example, Sweigart and Gross 1978 for the red giant branch). With a change of metal abundance, the tracks are displaced but almost retain their relative displacements. This behavior means that the displacement in $\log T_{\mathrm{eff}}$ in the H-R diagram, after correction to a fixed metal abundance, is a measure of the stellar mass. In principle, this displacement may be calibrated using the theoretical tracks. We used the Ca abundances given in Paper I to perform the correction relative to the solar Ca abundance.

The portion of the H-R diagram occupied by the G and K giants is shown in Figure 7. Lower luminosity ($M_{\mathrm{bol}} > +1.5$) giants and weak G band stars have not been plotted. Displacements in $\log T_{\mathrm{eff}}$ relative to the reference track and the Li abundances from Paper I are plotted in Figure 8. With the exception of a single transgressor (η Cet), the points in Figure 8 conform to a distribution with a well-defined upper boundary. Indeed, all but about four stars (η Cet, α Cas, ϵ Vir, and β Cet) scatter about a mean relation within a spread of about ± 0.6 dex; a few additional stars appear to have Li abundances below the mean line but plausible uncertainties in $\Delta \log T_{\mathrm{eff}}$ could restore them to the mean line. The scatter is generally consistent with the estimated Li and $\Delta \log T_{\mathrm{eff}}'$ uncertainties.

Figure 8 is surely new evidence that the stellar mass has a primary influence on the Li abundance in red giants. We have attempted a preliminary calibration of the Li-$\Delta \log T_{\mathrm{eff}}'$ relation. Three principal ingredients enter this calibration:

1. The evolutionary tracks computed by Sweigart and Gross (1978).

2. The assumption that the depletion of Li in main-sequence stars follows the equation

$$\epsilon(\mathrm{Li}) = \epsilon(\mathrm{Li})_0 \exp\left(-t/\tau_{\mathrm{Li}}\right)$$

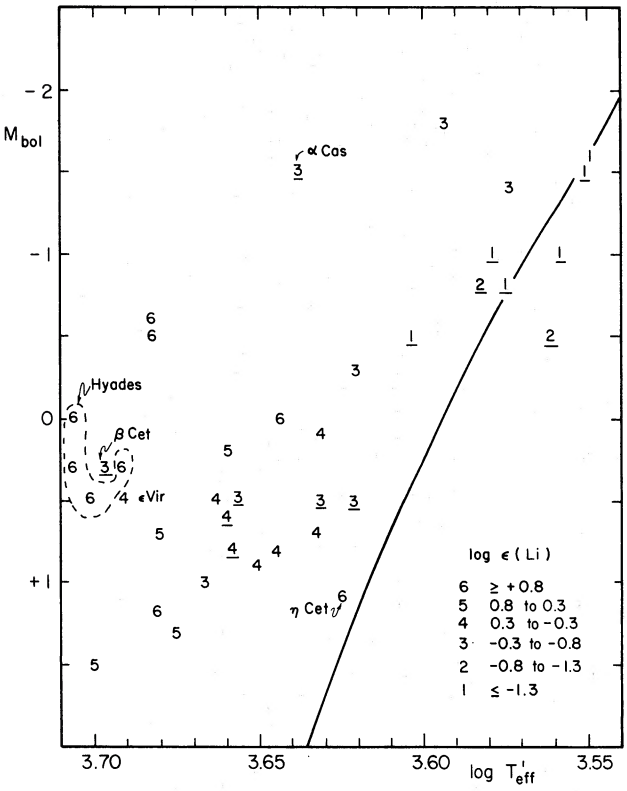

FIG. 7.—An H-R diagram showing the G and K giants from Paper I. The Li abundance class of the giants is indicated. This class number is underlined when an upper limit to the Li abundance was obtained. The solid line shows the predicted red giant branch (Sweigart and Gross 1978) for $\mathcal{M} = 0.9\ \mathcal{M}_\odot$ and a composition $X = 0.79$, $Y = 0.20$, $Z = 0.01$.

where $\epsilon(\mathrm{Li})_0$ is the initial or cosmic abundance [$\log \epsilon(\mathrm{Li})_0 = 3.0$, Boesgaard 1976]. We evaluate ϵ(Li) using the main-sequence lifetime and expect τ_{Li} to be between 1 and 2 Gyr where 1 Gyr = 10^9 yr with, perhaps, a weak dependence on stellar mass.

3. The predicted dilution factors for Li in red giants are taken from Iben (1967*a*, *b*).

In Figure 9, we compare the predicted and observed relations. The former have been normalized so that $\mathcal{M} \sim 1\ \mathcal{M}_\odot$ corresponds to $\Delta \log T_{\mathrm{eff}}' = 0$. Clearly, the predictions are only a fair match to the observations. Although agreement could be improved by introducing the decay time τ_{Li} as a mass-dependent quantity, one striking disagreement would remain; i.e., the observations in Figure 8 span a range of about 0.13 in $\Delta \log T_{\mathrm{eff}}'$, but the predicted range for 0.8 to 3 $\mathcal{M}_\odot$ is just about 0.06 dex; the observations are bounded by the Hyades ($\mathcal{M} \approx 2.0 \pm 0.3\ \mathcal{M}_\odot$, van den Heuvel 1975) and $\mathcal{M} \approx 0.9\ \mathcal{M}_\odot$ (the main sequence lifetime for $\mathcal{M} \lesssim 0.9\ \mathcal{M}_\odot$ exceeds the age of the galactic disk). An inability to separate red giants on the first and second ascents would stretch the prediction by about 0.02 dex. At the low end of the mass range, the sample probably contains an increasing number of giants on the first ascent

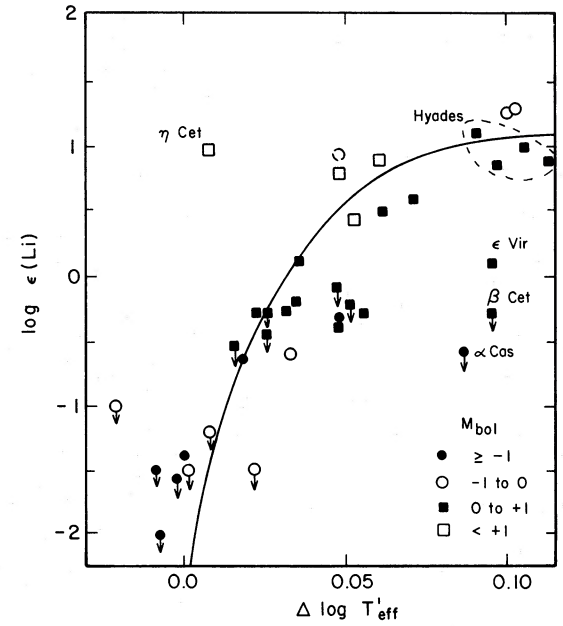

FIG. 8.—Li abundance in G and K giants vs. the displacement in the H-R diagram (Fig. 7) relative to the predicted track for $\mathcal{M} = 0.9\ \mathcal{M}_\odot$.

for which the Li will not be fully diluted. This selection effect must flatten the observed relation. The remaining discrepancy seems to be too large to be attributable entirely to the observational uncertainties. At the largest masses, clump giants suffering the full dilution of Li should dominate.

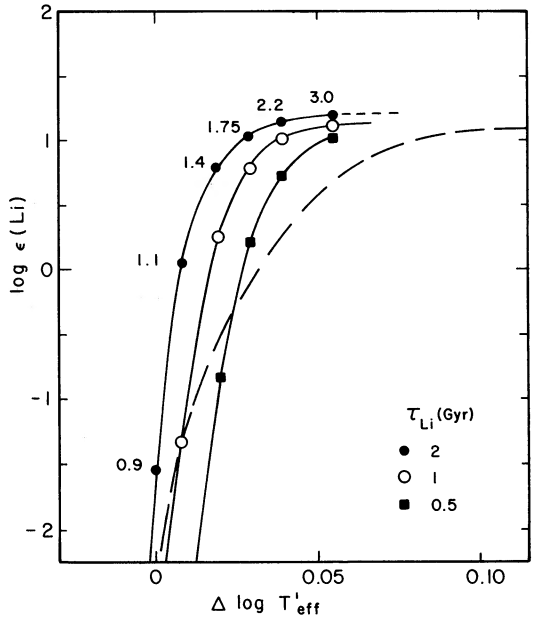

FIG. 9.—Predicted and observed relations between the Li abundance in G and K giants and the displacement $\Delta \log T_{\mathrm{eff}}$. The predictions are given for three decay times and masses 0.9, 1.1, 1.4, 1.75, 2.2, and 3.0 $\mathcal{M}_\odot$. The broken line is taken from Fig. 8 as the upper boundary to the observed points.

The members of the trio—ϵ Vir, β Cet, and α Cas—are marked by their low Li abundances. This same trio also stands out when the CNO abundances are examined (Lambert and Ries 1981). Apparently, these stars experienced an exceptional level of nuclear processing in the main-sequence phase. It is pleasing that the independent analyses of Li and CNO (with the $^{12}C/^{13}C$ ratio) point to the same conclusion. The other standout in Figure 8 is η Cet. Unfortunately, a CNO analysis has not been completed for this star, but the low $^{12}C/^{13}C$ ratio indicates that the star has been convectively mixed. Since Li is confined to a thin outer skin in a main-sequence star, Li depletion in a red giant should run ahead of the reduction in the $^{12}C/^{13}C$ ratio and, therefore, η Cet is difficult to fit into the standard model and simple variants of it. Perhaps the adopted absolute visual magnitude is in error; however, a change of 1.6 magnitudes is needed. Recently, Wallerstein and Sneden (1982) have discovered a Li-rich K giant. η Cet may be related to their discovery. A further search now needs to be undertaken to uncover additional examples of Li-rich giants and, then, to analyze their chemical composition for clues to their origin.

An application of the same procedure to the M giant sample is summarized in Figure 10. In Figure 10*a*, we show the displacements $\Delta \log T_{\rm eff}'$ corresponding to the metal (Al) abundance in Table 3. Figure 10*b* is constructed from the log $T_{\rm eff}$ displacements without the metal abundance correction. Note that at $M_{\rm bol} = -2$, the latter amounts to $\Delta \log T_{\rm eff} = 0.07$ for a 1 dex change in metal abundance. According to Figure 10, the M giants satisfy approximately the same Li abundance-mass relation as the G and K giants. The M giants are an extension to higher luminosity and lower effective temperature of the sample displayed in Figures 7 and 8. The bolometric magnitudes for the M giants span the range -1.0 to -3.2. Few of the G and K giants are more luminous than $M_{\rm bol} = -1$, and most are clustered about $M_{\rm bol} \approx +0.5$.

Application of the metal abundance dependent correction to $\Delta \log T_{\rm eff}$ results in an increased scatter in Figure 10*a* with several stars failing to fit the G and K giant relation; for example, δ Sge, δ Vir, and γ Eri. We suspect that the uncertainties in the metal abundance derived from the TiO line-blanketed spectra are responsible for the scatter. If the stars are supposed to have a similar abundance, they occupy a narrow interval in $\Delta \log T_{\rm eff}$ with just one outstanding example (δ Sge) failing above the G and K giant relation. Perhaps, δ Sge is a cool relative of η Cet. Alternatively, this difference could merely reflect a difference in the absolute magnitude. δ Sge is the only class II star included in the giants. Also, it is a spectroscopic binary (Batten, Fletcher, and Mann 1978) which could cause problems with the absolute magnitude determination. Tsuji (1981) has already noted that the M giants cluster around a single track in the H-R diagram. If Figure 10*b* is appropriate, the Li abundances suggest that the M giants have masses $\mathcal{M} \lesssim 2\,\mathcal{M}_\odot$. There is no evidence from this sample and the extended sample inspected at low dispersion by Merchant (1967) for Li-enrichment related to a dredge-up of C-rich material for the He-burning shell.

Modest extensions of our survey are likely to shed more light on the nuclear processing and mixing affecting the M giants. Clearly, the metal abundance should be derived from atomic lines in near-infrared regions unaffected by TiO and other molecular line-blanketing. A combination of the Li abundance with a full CNO

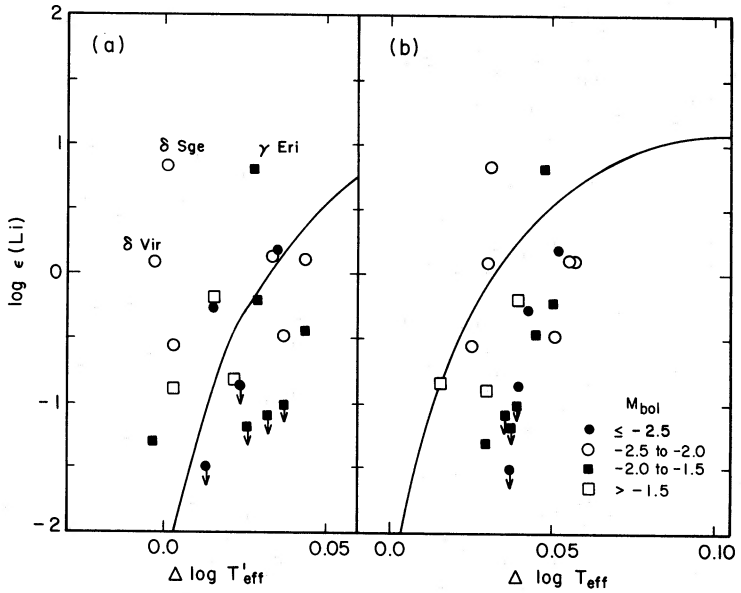

FIG. 10.—Li abundance in M giants vs. the displacement in the H-R diagram relative to the $\mathcal{M} = 0.9\,\mathcal{M}_\odot$ track. In Fig. 10*a*, the displacements, $\Delta \log T_{\rm eff}'$, have been adjusted for the observed metal (Al) abundance. Fig. 10*b* uses the direct displacements, log $T_{\rm eff}$, computed from the adopted $T_{\rm eff}$ (Table 1). The solid line in both panels is the mean relation for the G and K giants from Fig. 8.

element and isotope analysis must increase the pool of information. In order to probe the stars enriched with freshly dredged-up carbon, the Li abundance analysis must be pushed to lower effective temperatures. This for the M stars means even stronger TiO blanketing at 6707 Å. Perhaps subordinate lines at 6103 Å and 8126 Å should be considered. Merchant (1967) noted that the former was visible in her spectra of δ Sge.

We should like to thank the Louisiana State University Network Computer Center for providing the large amount of computer time necessary for the completion of this project. We thank Dr. J. Tomkin for assistance at the telescope and Mr. J. F. Dominy for assistance in the reduction of the spectra. This work was supported at LSU by NSF grants 78-25538 and 80-23232 and at the University of Texas by NSF grant 79-22014 and the Robert A. Welch Foundation.

REFERENCES

Arnold, J. O., and Nicholls, R. W. 1972, *J. Quant. Spectrosc. Rad. Transf.*, **12**, 1435.
Auer, L. H., Heasley, J. R., and Milkey, R. W. 1972, *Kitt Peak Obs. Contrib.*, 555.
Auman, J. R., and Woodrow, J. E. J. 1975, *Ap. J.*, **197**, 163.
Batten, A. H., Fletcher, J. M., and Mann, P. J. 1978, *Pub. Dom. Ap. Obs.*, **15**, No. 5.
Bell, R. A., and Gustafsson, B. 1978, *Astr. Ap. Suppl.*, **34**, 229.
Bernat, A. P., Hall, D. N. B., Hinkle, K. H., and Ridgway, S. T. 1979, *Ap. J. (Letters)*, **233**, L135.
Blanco, V. M., Demers, S., Douglass, G. G., and Fitzgerald, M. P. 1970, *Pub. US Naval Obs.*, **21**.
Boesgaard, A. M. 1970, *Ap. Letters*, **5**, 145.
———. 1976, *Pub. A.S.P.*, **88**, 353.
Cassinelli, J. P. 1979, *Ann. Rev. Astr. Ap.*, **17**, 275.
Clegg, R. E. S., Lambert, D. L., and Bell, R. A. 1979, *Ap. J.*, **234**, 188.
Collins, J. G., and Faÿ, T. D. 1974, *J. Quant. Spectrosc. Rad. Transf.*, **14**, 427.
Davis, S. P., and Phillips, J. G. 1963, *The Red System* ($A^2\Pi$–$X^2\Sigma$) *of the CN Molecule* (Berkeley: University of California Press).
Delbouille, L., Neven, L., and Roland, D. 1973, *Photometric Atlas of the Solar Spectrum from 3800 to 10,000 Å* (Liège: Université de Liège).
Duncan, D. K. 1981, *Ap. J.*, **248**, 651.
Gustafsson, B., and Bell, R. A. 1979, *Astr. Ap.*, **74**, 313.
Gustafsson, B., Bell, R. A., Eriksson, K., and Nordlund, Å. 1975, *Astr. Ap.*, **43**, 407.
Herbig, G. H. 1965, *Ap. J.*, **141**, 588.
Hinkle, K. H., Lambert, D. L., and Snell, R. L. 1976, *Ap. J.*, **210**, 684.
Hoffleit, D. 1964, *Catalogue of Bright Stars* (New Haven: Yale University Observatory Press).
Holweger, H. 1967, *Zs. Ap.*, **65**, 365.
Holweger, H., and Müller, E. A. 1974, *Solar Phys.*, **39**, 19.
Iben, I. 1966, *Ap. J.*, **143**, 483.
———. 1967*a*, *Ap. J.*, **147**, 624.
———. 1967*b*, *Ap. J.*, **147**, 650.
Johnson, H. L. 1966, *Ann. Rev. Astr. Ap.*, **4**, 193.
Johnson, H. L., Mitchell, R. I., Iriarte, B., and Wisniewski, W. Z. 1966, *Pub. Lunar and Planet Lab.*, **4**, 99.
Johnson, H. R., Bernat, A. P., and Krupp, B. 1980, *Ap. J. Suppl.*, **42**, 501.
Johnson, H. R., Collins, J. G., Krupp, B., and Bell, R. A. 1977, *Ap. J.*, **212**, 760.
Kurucz, R. L., and Peytremann, E. 1975, *Smithsonian Ap. Obs. Spec. Rept.*, 362.
Lambert, D. L., Brown, J. A., Hinkle, K. H., and Johnson, H. R. 1981, in preparation.
Lambert, D. L., Dominy, J. F., and Sivertsen, S. 1980, *Ap. J.*, **235**, 114 (Paper I).
Lambert, D. L., and Luck, R. E. 1978, *M.N.R.A.S.*, **183**, 79.
Lambert, D. L., and Ries, L. M. 1981, *Ap. J.*, **248**, 228.
Luck, R. E. 1977, *Ap. J.*, **218**, 752.
Luck, R. E., and Bond, H. E. 1980, *Ap. J.*, **241**, 218.
Merchant, A. 1967, *Ap. J.*, **147**, 587.
Moore, C. E., Minnaert, M. G. J., and Houtgast, J. 1966, *NBS Monog.*, 61.
Mutschlechner, J. P., and Keller, C. F. 1972, *Solar Phys.*, **22**, 70.
Neugebauer, G., and Leighton, R. B. 1969, *NASA Special Pub.*, 3047.
Paczyński, B. 1970, *Acta Astr.*, **20**, 47.
Phillips, J. G. 1973, *Ap. J. Suppl.*, **26**, 313.
Price, M. C., Sulzman, K. G. P., and Penner, S. S. 1974, *J. Quant. Spectrosc. Rad. Transf.*, **14**, 1273.
Ramsey, L. W. 1977, *Ap. J.*, **215**, 827.
———. 1981, *Ap. J.*, **245**, 984.
Ridgway, S. T., Joyce, R. R., White, N. M., and Wing, R. F. 1980, *Ap. J.*, **235**, 126.
Schatzman, E. 1977, *Astr. Ap.*, **56**, 211.
Straus, J. M., Blake, J. B., and Schramm, D. N. 1976, *Ap. J.*, **204**, 481.
Sweigart, A. V., and Gross, P. G. 1978, *Ap. J. Suppl.*, **36**, 405.
Tsuji, T. 1981, *Astr. Ap.*, **99**, 48.
van den Heuvel, E. P. J. 1975, *Ap. J. (Letters)*, **196**, L121.
Vogt, S. S., Tull, R. G., and Kelton, P. K. 1978, *Appl. Optics*, **17**, 574.
Wallerstein, G., and Sneden, C. 1982, *Ap. J.*, **255**, 577.
White, N. M. 1980, *Ap. J.*, **242**, 646.
Whiting, E. E. 1972, NASA Technical Note, D-7268.
Wiese, W. L., Smith, M. W., and Glennon, B. M. 1966, *Atomic Transition Probabilities*, Vol. **1** (NSRDS-NBS 4).
Wilson, O. C. 1976, *Ap. J.*, **205**, 823.
Zappala, R. R. 1972, *Ap. J.*, **172**, 57.

DAVID L. LAMBERT: Department of Astronomy, University of Texas at Austin, Austin, TX 78712

R. EARLE LUCK: Department of Physics and Astronomy, Louisiana State University, Baton Rouge, LA 70803